SymC and the QFT: Critical-Damping Boundary Dynamics of Dissipative Quantum Fields v2

Nate Christensen

Symmetry Universe Project, Missouri, USA

17 November 2025

Abstract

Version 2 clarifies the role of the $\chi = 1$ boundary, adds the information-efficiency interpretation, incorporates the inheritance mechanism as a structural constraint, and removes material not directly related to dissipative quantum fields.

Symmetrical Convergence (SymC) identifies the dimensionless ratio $\chi \equiv \gamma/(2|\omega|)$ as a structural boundary separating oscillatory and monotone dynamics in open quantum systems. At $\chi = 1$, each field mode reaches a non-Hermitian Exceptional Point (EP), where the retarded propagator's poles coalesce and the causal response function becomes $g(t) = \Theta(t)\, te^{-|\omega|t}$. This manuscript provides the complete open-QFT formulation of SymC, including theoretical foundations, covariance, substrate inheritance, renormalization-group stability, non-Markovian EP broadening, interpretation of the damping transition, and quantitative laboratory falsification. The analysis emphasizes the structural role of the $\chi = 1$ boundary as both a dynamical separatrix and an information-efficiency extremum, and shows that it remains robust under substrate inheritance, weak renormalization-group flow, and controlled non-Markovian broadening.

1 Modeling Assumptions and Scope

For a scalar field $\phi(x)$ weakly coupled to an environment, integrating out the bath degrees of freedom through influence-functional techniques yields the effective equation

$$(\Box + m^2)\phi + \gamma(u \cdot \partial)\phi = 0, \tag{1}$$

where γ is a dissipative damping rate and u^μ the bath four-velocity. This form applies in the regime of weak coupling, short memory, and negligible spatial gradients in bath correlations. Closed quantum field theories without environmental interaction are outside the scope of SymC. The present work treats open QFTs where irreversible damping is physically realized. This framework builds upon the SymC interpretation of the electromagnetic vacuum as an effectively lossless $\chi = 0$ photon substrate; the present analysis characterizes the $\chi = 1$ interaction boundary that emerges when those fields couple to a dissipative environment.

2 Field-Mode Dynamics and the SymC Discriminant

Fourier-decompose the field

$$\phi(x) = \int \frac{d^3k}{(2\pi)^3}\, q_k(t)\, e^{i\mathbf{k}\cdot\mathbf{x}}. \tag{2}$$

The mode equation of motion is

$$\ddot{q}_k + \gamma_k \dot{q}_k + \omega_k^2 q_k = 0, \qquad \omega_k^2 = k^2 + m_{\text{eff}}^2. \tag{3}$$

Define the SymC ratio

$$\chi_k \equiv \frac{\gamma_k}{2|\omega_k|}. \tag{4}$$

Then

- $\chi_k < 1$: underdamped, oscillatory;
- $\chi_k = 1$: critical damping, EP;
- $\chi_k > 1$: overdamped, monotone.

The discriminant $\Delta_k = \gamma_k^2 - 4\omega_k^2$ encodes these regimes.

3 Exceptional Point and Spectral Signature

The retarded propagator is

$$G_k^R(\Omega) = \frac{1}{-\Omega^2 - i\gamma_k\Omega + \omega_k^2}. \tag{5}$$

The poles are

$$\Omega_\pm = -\frac{i\gamma_k}{2} \pm \sqrt{\omega_k^2 - \frac{\gamma_k^2}{4}}. \tag{6}$$

At $\chi_k = 1$ the poles coalesce at $\Omega = -i|\omega_k|$, producing the EP. The corresponding causal kernel is

$$g_k(t) = \Theta(t)\, t e^{-|\omega_k|t}. \tag{7}$$

This kernel has no oscillatory component, defines a single relaxation timescale, and encodes the fastest non-oscillatory decay. The spectral function

$$A_k(\Omega) = \frac{\gamma_k\Omega}{\left(\omega_k^2 - \Omega^2\right)^2 + \gamma_k^2\Omega^2}, \tag{8}$$

exhibits two peaks for $\chi_k < 1$ and a merged zero-detuning peak for $\chi_k \approx 1$.

4 Covariance of the SymC Condition

Including a bath velocity u^μ, the inverse propagator becomes

$$D(k) = -\left(k^2 - m^2\right) - i\gamma(k \cdot u). \tag{9}$$

Thus the EP condition is covariant:

$$\gamma = 2|k \cdot u|. \tag{10}$$

For any fixed mode, the truth of this condition is frame-independent. However, different inertial frames identify different sets of modes as critical due to transformations of k^μ.

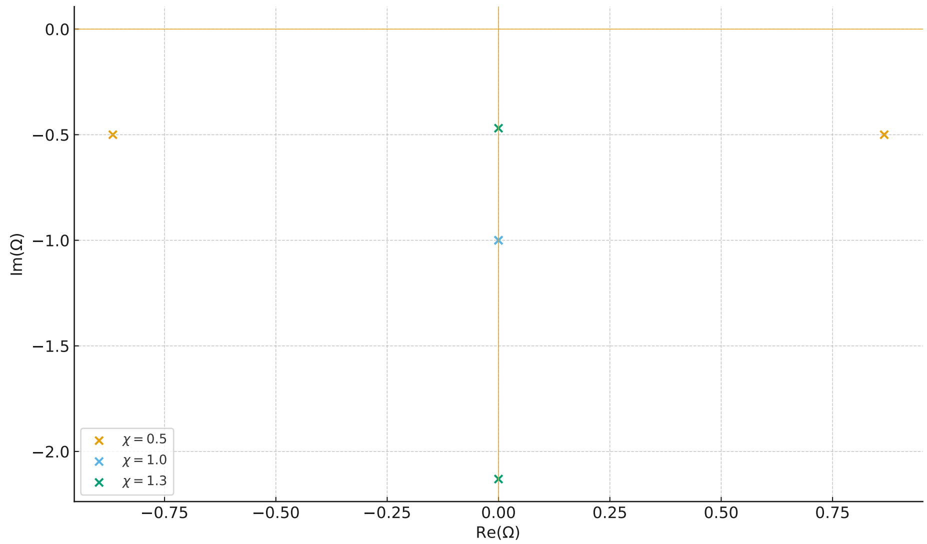

Figure 1: Pole structure of the damped mode as the SymC ratio $\chi_k = \gamma_k/(2|\omega_k|)$ is varied. For $\chi_k < 1$ the retarded propagator has two complex-conjugate poles with nonzero real parts (underdamped regime). At $\chi_k = 1$ the poles coalesce at $\Omega = -i|\omega_k|$, reaching the $\chi_k = 1$ critical-damping point (an Exceptional Point, EP). For $\chi_k > 1$ both poles lie on the imaginary axis and dynamics become strictly monotone.

5 Information-Efficiency Extremum

The $\chi = 1$ boundary is not just a dynamical feature but a thermodynamic optimum. Within this setting, an information-efficiency functional is defined as

$$\eta(\chi) \equiv \frac{I(\chi)}{\Sigma(\chi)}, \tag{11}$$

representing the ratio of information throughput I to entropy production Σ. Within the broader SymC framework, this functional $\eta(\chi)$ attains a strict local maximum at $\chi = 1$:

- For $\chi < 1$ (underdamped), the system "rings," wasting energy in persistent oscillations and corrupting information with overshoot and ringing artifacts.
- For $\chi > 1$ (overdamped), the system is rigid and relaxes slowly, sacrificing responsiveness and information throughput for excessive stability.

The $\chi = 1$ boundary is therefore the unique state of maximal efficiency, achieving the fastest, most stable response for a given energetic cost. This provides a physical *purpose* for the boundary's selection: systems driven by dynamical and thermodynamic pressures are steered toward this near-optimal operating point.

6 Substrate Inheritance: Mechanism and Stability

6.1 Mechanism

Within the broader SymC program, *Substrate Inheritance* is the principle that stable, complex systems at a macroscopic scale L cannot be built from persistently unstable, "ringing" substrates

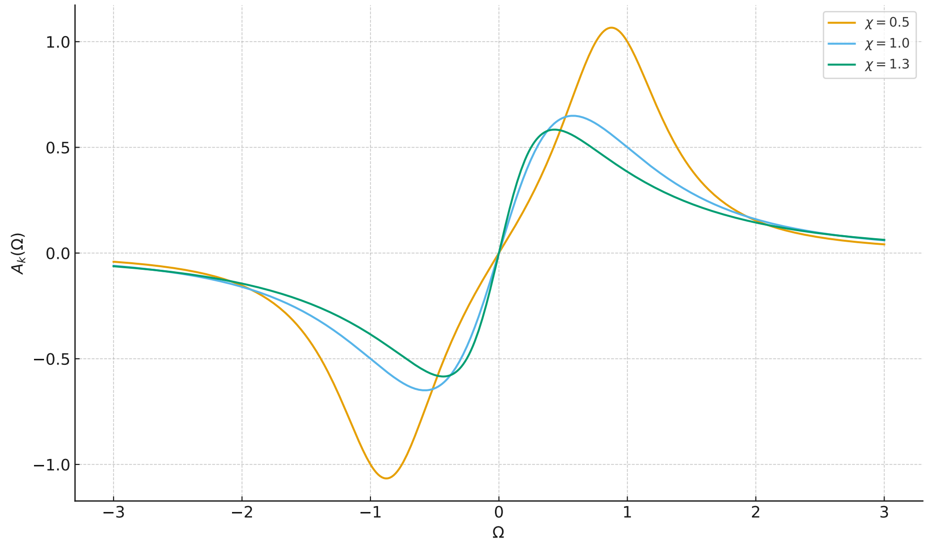

Figure 2: Spectral function $A_k(\Omega)$ for a single mode at three values of the SymC ratio: $\chi_k = 0.5$ (underdamped doublet), $\chi_k = 1.0$ (merged peak at zero detuning), and $\chi_k = 1.3$ (overdamped single peak). The zero-detuning peak merger at $\chi_k \approx 1$ provides the primary experimental falsifier.

at the microscopic QFT scale $L - 1$. Dynamical and physical constraints naturally bias foundational QFT substrates toward stabilization in the near-critical adaptive window ($0.8 \lesssim \chi \lesssim 1.0$). This damping structure is then inherited by higher-level dynamical systems, regardless of physical domain, whenever stability constraints impose analogous response requirements.

6.2 Stability

Substrate inheritance introduces shifts

$$\omega \to \omega + \delta\omega, \qquad \gamma \to \gamma + \delta\gamma. \tag{12}$$

Thus

$$\delta\chi = \chi \left(\frac{\delta\gamma}{\gamma} - \frac{\delta\omega}{\omega} \right). \tag{13}$$

In inheritance models, the same structural features of the substrate typically renormalize ω and γ proportionally,

$$\frac{\delta\gamma}{\gamma} = \frac{\delta\omega}{\omega} + \mathcal{O}(\varepsilon^2), \tag{14}$$

so

$$\delta\chi = \mathcal{O}(\varepsilon^2). \tag{15}$$

Thus $\chi = 1$ is a stable, self-consistent condition under substrate perturbations, with deviations only entering at second order.

7 Renormalization-Group Stability

A toy RG model with quartic coupling λ yields

$$\frac{d\chi}{d\ell} = -\frac{5\lambda}{64\pi^2}\,\chi. \tag{16}$$

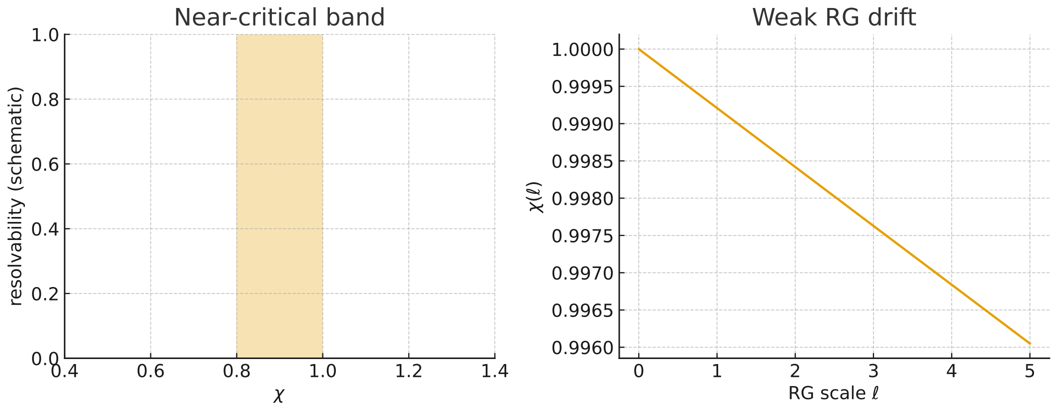

Figure 3: Left: schematic representation of the near-critical adaptive window in the SymC ratio, $0.8 \lesssim \chi \lesssim 1.0$, arising from finite-memory broadening in non-Markovian environments. Right: illustrative renormalization-group flow of χ in a toy ϕ^4 model at weak coupling ($\lambda \sim 0.1$), showing that χ drifts by less than 1% across several decades in energy scale. Together these panels support the picture of $\chi = 1$ as a structurally stable, near-fixed manifold that operationally appears as a narrow band.

For weak coupling $\lambda \sim 0.1$, χ changes by less than 1% across three decades of scale. Thus $\chi = 1$ remains approximately invariant under scale evolution and constitutes a robust near-fixed manifold in the weak-coupling regime.

8 Non-Markovian Memory and the Near-Critical Band

Let the memory kernel be

$$K(t) = \gamma_0 e^{-\Gamma t}. \tag{17}$$

Then

$$\gamma_{\text{eff}}(\omega, \Gamma) = \gamma_0 \sqrt{1 + (\omega/\Gamma)^2}. \tag{18}$$

For $\Gamma \gg |\omega|$, the Markovian limit is recovered. For $\Gamma \sim |\omega|$, frequency-dependent damping causes the EP to broaden into a near-critical band

$$0.8 \lesssim \chi \lesssim 1.0. \tag{19}$$

In long-memory regimes ($\Gamma \ll |\omega|$) the EP becomes a smooth crossover, though the peak-merger diagnostic remains detectable if instrumental resolution is sufficient.

9 Experimental Protocol and Quantitative Falsifier

Circuit QED provides tunable γ via Purcell coupling:

$$\gamma \approx \kappa_{\text{ext}} + \kappa_{\text{int}}. \tag{20}$$

A minimal falsification protocol proceeds as follows:

1. Tune χ from 0.5 to 1.5 by adjusting the external coupling.

2. Measure $S_{11}(\Omega)$ or transmission as a function of frequency.

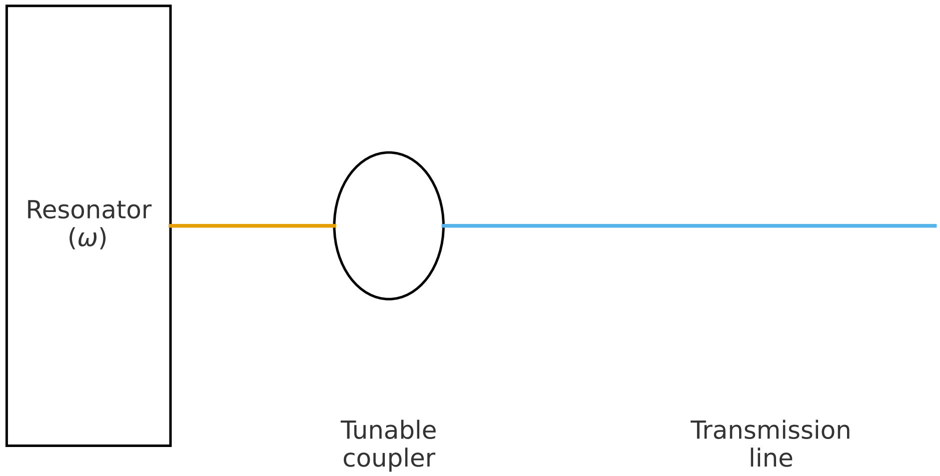

Figure 4: Conceptual circuit-QED implementation of the SymC falsifier. A superconducting resonator of frequency ω is coupled to an external transmission line with tunable coupling κ_{ext}, giving a total damping rate $\gamma \simeq \kappa_{\text{ext}} + \kappa_{\text{int}}$. Sweeping κ_{ext} tunes the SymC ratio $\chi = \gamma/(2|\omega|)$ from underdamped to overdamped. The predicted doublet-to-singlet spectral transition near $\chi \approx 1$ provides a decisive test; failure to observe a peak merger in the window $0.8 \leq \chi \leq 1.0$, at sufficient spectral resolution, falsifies the SymC boundary claim for this platform.

3. Fit the resulting spectra to one-peak versus two-peak models.

Failure to observe peak merger within $0.8 \leq \chi \leq 1.0$ with resolution $\delta\Omega \lesssim 0.01\omega$ rules out SymC for that system.

10 Decoherence and Temperature Dependence

Lindblad channels that produce γ also cause coherence decay. For $\chi < 1$, oscillations retain partial phase coherence. For $\chi > 1$, coherence collapses before a full oscillation. At $\chi = 1$, both decay rates coincide. Thermal baths raise $\gamma(T)$, shifting systems along the SymC axis. The SymC classification applies at the realized $\gamma(T)$.

11 Discussion

SymC provides a structurally well-defined and falsifiable boundary for open QFT dynamics. Its stability under inheritance, weak RG drift, and finite memory effects establishes the EP as a structural feature of open quantum fields. The framework unifies dynamical stability, thermodynamic efficiency, and experimental accessibility. The appearance of this QFT boundary across scales is a structural consequence of the SymC framework rather than an analogy.

References

[1] H.-P. Breuer and F. Petruccione, *The Theory of Open Quantum Systems* (Oxford University Press, 2002).

[2] V. Gorini, A. Kossakowski, and E. C. G. Sudarshan, "Completely Positive Dynamical Semigroups of N-Level Systems," J. Math. Phys. **17**, 821 (1976).

[3] G. Lindblad, "On the Generators of Quantum Dynamical Semigroups," Commun. Math. Phys. **48**, 119 (1976).

[4] A. O. Caldeira and A. J. Leggett, "Quantum Tunneling in a Dissipative System," Ann. Phys. **149**, 374 (1983).

[5] U. Weiss, *Quantum Dissipative Systems* (World Scientific, 1999).

[6] C. M. Bender and S. Boettcher, "Real Spectra in Non-Hermitian Hamiltonians Having PT Symmetry," Phys. Rev. Lett. **80**, 5243 (1998).

[7] W. D. Heiss, "The Physics of Exceptional Points," J. Phys. A: Math. Theor. **45**, 444016 (2012).

[8] Y. Ashida, Z. Gong, and M. Ueda, "Non-Hermitian Physics," Adv. Phys. **69**, 3 (2020).

[9] A. A. Clerk, M. H. Devoret, S. M. Girvin, F. Marquardt, and R. J. Schoelkopf, "Introduction to Quantum Noise, Measurement, and Amplification," Rev. Mod. Phys. **82**, 1155 (2010).

[10] I. Nakamura and F. Nori, "Open Quantum Field Theories and Dissipative Bosonic Fields," Phys. Rev. A **98**, 012105 (2018).

[11] L. V. Keldysh, "Diagram Technique for Nonequilibrium Processes," Sov. Phys. JETP **20**, 1018 (1965).

[12] L. M. Sieberer, M. Buchhold, and S. Diehl, "Keldysh Field Theory for Driven Open Quantum Systems," Rep. Prog. Phys. **79**, 096001 (2016).